Changes in growing season duration and productivity of northern vegetation inferred from long-term remote sensing data

Environmental Research Letters

LETTER

Changes in growing season duration and productivity of northern vegetation inferred from long-term remote sensing data

Taejin Park[1], Sangram Ganguly[2], Hans Tømmervik[3], Eugénie S Euskirchen[4], Kjell-Arild Høgda[5], Stein Rune Karlsen[5], Victor Brovkin[6], Ramakrishna R Nemani[7] and Ranga B Myneni[1]

1   Department of Earth and Environment, Boston University, Boston, MA 02215, USA
2   Bay Area Environmental Research Institute, NASA Ames Research Center, Moffett Field, CA 94035, USA
3   Norwegian Institute for Nature Research, FRAM−High North Centre for Climate and the Environment, PO Box 6606 Langnes, N-9296 Tromsø, Norway
4   Institute of Arctic Biology, University of Alaska Fairbanks, Fairbanks, Alaska, USA
5   Norut, PO Box 6434, N-9294 Tromsø, Norway
6   Max Planck Institute for Meteorology, Hamburg, Germany
7   NASA Advanced Supercomputing Division, NASA Ames Research Center, Moffett Field, CA 94035, USA

E-mail: parktj@bu.edu

Abstract

Monitoring and understanding climate-induced changes in the boreal and arctic vegetation is critical to aid in prognosticating their future. We used a 33 year (1982–2014) long record of satellite observations to robustly assess changes in metrics of growing season (onset: SOS, end: EOS and length: LOS) and seasonal total gross primary productivity. Particular attention was paid to evaluating the accuracy of these metrics by comparing them to multiple independent direct and indirect growing season and productivity measures. These comparisons reveal that the derived metrics capture the spatio-temporal variations and trends with acceptable significance level (generally $p < 0.05$). We find that LOS has lengthened by 2.60 d dec^{-1} ($p < 0.05$) due to an earlier onset of SOS (-1.61 d dec^{-1}, $p < 0.05$) and a delayed EOS (0.67 d dec^{-1}, $p < 0.1$) at the circumpolar scale over the past three decades. Relatively greater rates of changes in growing season were observed in Eurasia (EA) and in boreal regions than in North America (NA) and the arctic regions. However, this tendency of earlier SOS and delayed EOS was prominent only during the earlier part of the data record (1982–1999). During the later part (2000–2014), this tendency was reversed, i.e. delayed SOS and earlier EOS. As for seasonal total productivity, we find that 42.0% of northern vegetation shows a statistically significant ($p < 0.1$) greening trend over the last three decades. This greening translates to a 20.9% gain in productivity since 1982. In contrast, only 2.5% of northern vegetation shows browning, or a 1.2% loss of productivity. These trends in productivity were continuous through the period of record, unlike changes in growing season metrics. Similarly, we find relatively greater increasing rates of productivity in EA and in arctic regions than in NA and the boreal regions. These results highlight spatially and temporally varying vegetation dynamics and are reflective of biome-specific responses of northern vegetation during last three decades.

1. Introduction

Boreal and arctic ecosystems cover 22% of the terrestrial surface and stretch over North America (NA) and Eurasia (EA). They play a crucial role in the Earth system by regulating energy–water–carbon exchanges between the land surface and the planetary boundary layer (Chapin *et al* 2000). During the last half-century, these regions have experienced temperature increases of 0.3 °C–1.0 °C per decade higher

than anywhere else on the Earth, particularly during the winter and spring seasons (Solomon 2007). A changing thermal regime and its consequences on physical, hydrological and biogeochemical conditions such as snow depth, soil moisture, disturbance etc. have already affected northern vegetation structure and function (Walther *et al* 2002). For example, increasing shrub cover across a broad range of hemispheric tundra area, termed as '*shrubification*', has been documented (Tape *et al* 2006) and changing tree growth has been observed in NA boreal forests (Beck *et al* 2011). As these changes may feedback on regional and global climate, an accurate characterization of changes during the recent past and some idea of future changes is a critical topic of research.

As a way to diagnose vegetation response to climate change, monitoring growing season duration and productivity has drawn particular attention because these are sensitive and easily measurable indicators (Richardson *et al* 2013). Field studies have indicated that the growing season duration for northern vegetation has significantly increased over the past decades due to both an earlier start and delayed ending (Parmesan and Yohe 2003, Menzel *et al* 2006). This is generally thought to result in a longer carbon assimilation period due to relaxation of low temperature limits on metabolism (Nemani *et al* 2003), and in turn an increase in primary productivity (Xu *et al* 2013, Forkel *et al* 2016). Indeed, ground observations confirm enhanced productivity from a lengthened photosynthetically active period (Richardson *et al* 2010, Keenan *et al* 2014).

Satellite observations have been employed to monitor and understand changes in growing season duration and productivity at large spatial scales. Remote sensing data reveal widespread lengthening of the growing season and an increase in gross primary productivity, also called 'greening', both of which are associated with warmer air temperatures in the high latitudes during 1980s and 1990s (Myneni *et al* 1997). After this period, divergent responses in productivity between boreal (decrease in productivity called 'browning') and arctic (contiguous greening) vegetation (Goetz *et al* 2005, Piao *et al* 2011, Bjerke *et al* 2014), and a reduced or reversed rate of regional growing season changes were also reported (Høgda *et al* 2013, Wang *et al* 2015). Furthermore, asymmetric seasonal warming (Serreze *et al* 2000) and a multitude of drivers greatly complicate the characterization of variations in growing season duration and productivity. This complexity justifies the need for a comprehensive examination of the magnitude and direction of changes across the northern hemispheric landscape using the longest satellite data set currently available.

The primary objectives of this study are to: (1) evaluate the reliability of long-term growing season duration and productivity metrics inferred from satellite data, (2) investigate the spatiotemporal pattern and trend of changes in growing season duration and productivity, and (3) quantify changes across continents (EA and NA), biomes (arctic and boreal) and vegetation types. To achieve these objectives, we used a satellite dataset covering the northern high latitude region (>45°N) for the period 1982–2014 (33 years long). We first define pixel-wise growing season duration and productivity metrics, then introduce independent datasets to assess the reliability of metrics inferred from satellite data. Robust statistical tests and trend analyses are used to evaluate long-term vegetation dynamics.

2. Materials and methods

This study is focused on vegetation in the boreal and arctic regions depicted in figure S1. We define 12 sub-vegetation classes and 4 vegetation groups using the Moderate Resolution Imaging Spectroradiometer (MODIS) International Geosphere-Biosphere Programme land cover (Friedl *et al* 2010) and Circumpolar Arctic Vegetation Map (CAVM, Walker *et al* 2005). Details for vegetation map can be found in SI section 1. All data sets used in this study are briefly described in SI data section and their spatial resolutions are identically harmonized into 1/12° for comparison purpose.

2.1. Determination of long-term (33 year) growing season and productivity

Normalized difference vegetation index (NDVI) is a radiometric measure of the amount of photosynthetically active radiation (∼400–700 nm) absorbed by vegetation. It is calculated from contrasting reflectances at near-infrared (ρ_{nir}) and red (ρ_{red}) bands: $NDVI = (\rho_{nir} - \rho_{red})/(\rho_{nir} + \rho_{red})$ (Tucker 1979). NDVI has been widely used in studies of phenology, productivity, biomass and disturbance monitoring as it has been proven to be a good surrogate of vegetation photosynthetic activity (Pettorelli *et al* 2005). Here, we used the latest version of Global Inventory Modeling and Mapping Studies (GIMMS) NDVI dataset (NDVI3g) which is spanning from July 1981 to December 2014 with a native resolution of 1/12° at bimonthly time steps (Pinzon and Tucker 2014).

The growing season summed NDVI (or, GSSNDVI) has been found to be a good proxy for vegetation gross primary productivity (Goward *et al* 1985, Wang *et al* 2004). We derived long-term GSSNDVI from 1982 to 2014 through the inferred corresponding growing season metrics: onset, end and length of growing season (SOS, EOS and LOS, respectively). Two preprocessing steps were first performed to maintain distinct seasonal vegetation trajectory and minimize spurious signals (e.g., cloud and snow): (1) implementing the Savitzky–Golay filter to smooth the NDVI3g time series (Chen *et al* 2004, Jönsson and Eklundh 2004); (2) identifying background NDVI and replacing NDVI that varied irregularly during the

winter period (e.g., Beck *et al* 2006). After that, we linearly interpolated the dataset to a daily time step. We also use the daily freeze/thaw (FT) state of the ground to define the photosynthetically active period because vegetation may remain green during the dormant season (SI section 2.9).

Based on the daily NDVI and FT time series, we define pixel-wise photosynthetically active growing season metrics as follows (figure S2, Zhu *et al* 2016): (a) SOS is the day when the NDVI value is greater than 0.1 and has increased by 25% of the growing season amplitude; (b) EOS is the day when the NDVI value is greater than 0.1 and has decreased by 25% of the growing season amplitude; (c) the ground should be in thawed state; (d) LOS is the duration between SOS and EOS. Based on extracted growing season, the pixel-wise GSSNDVI for each grid (p) and year (y) can be calculated by cumulating daily NDVI ($f_{NDVI}(t)$) over LOS as below

$$\text{GSSNDVI}_{(p,y)} = \sum_{\text{SOS}_{(p,y)}}^{\text{EOS}_{(p,y)}} f_{\text{NDVI}}(t)_{(p,y)}. \quad (1)$$

2.2. Evaluation of growing season and productivity

We used several independent datasets to evaluate the reliability of inferred SOS, EOS, LOS and GSSNDVI metrics. For growing season metrics, we utilized three different sets of growing season metrics from MODIS products: standard land surface phenology product (MCD12Q2, 2001–2012, see SI section 2.2) and independently derived two NDVI (MOD13C1 and MCD43C4, 2000–2014, see SI sections 2.3–4) based growing season metrics via same method used in NDVI3g. Additionally, we used growing season metrics derived from flux tower measurements of gross primary productivity (GPP; figure S2, SI section 2.5). Similarly, to evaluate the NDVI3g based GSSNDVI, we used flux tower GPP, the MODIS GPP product (MOD17A3, 2000–2014, SI section 2.6), and a GPP product based on Multi-Tree Ensemble (MTE) approach from the Max Planck Institute (MTE-GPP, 1982–2011, SI section 2.7). Temperature based potential SOS (PSOS), EOS (PEOS), LOS (PLOS) and growing season summed warmth index (GSSWI) were also used (see SI section 2.10) as the temporal coverage, i.e. number of years, of other evaluation datasets was limited.

The cross-comparisons were performed at both site and continental scales. For site scale evaluation, we selected 109 sample sites based on the latest Benchmark Land Multisite Analysis and Intercomparison of Products (BELMANIP-2) scheme as it provided a good sampling across biomes and land surface types (Baret *et al* 2006). In flux tower versus satellite data comparisons, valid flux sites and data were ascertained as follows: (i) more than 95% of the days had daily GPP data, and (ii) the mean daily quality flag was more than 0.75 (Richardson *et al* 2010). For continental

scale comparisons, all the metrics were converted to anomalies with respect to their common period and then spatially averaged over North America (NA), Eurasia (EA) and the entire circumpolar (CP) region.

2.3. Quantification of growing season and productivity change

We used Vogelsang's $t-PS_T$ test (significance level of 0.1) to evaluate the 33 year temporal trends in growing season and productivity metrics. This method is a robust model for trend estimation and does not require *a priori* knowledge of stationarity and also avoids estimation of autocorrelation parameters (Vogelsang 1998). We also assessed trends with the Mann-Kendall test (Mann 1945), but these results are not presented as they were largely similar to those using the Vogelsang's method. In view of a hiatus in warming in the recent years (Trenberth and Fasullo 2013), the analysis was also performed separately for the early (1982–1999) and later (2000–2014) periods to compare with the entire period of data record (1982–2014).

3. Results and discussion

3.1. Evaluation of NDVI3g based growing season and productivity metrics

The NDVI3g based metrics of growing season (SOS, EOS and LOS) and seasonal total productivity (GSSNDVI) agree well with corresponding metrics derived from other evaluation datasets (table 1 and figures 1 and 2). Table 1 provides a summary of comparison for the 109 BELMANIP-2 sites distributed over the northern vegetated lands. The correspondence between NDVI3g based metrics and those from the improved MODIS NDVI (MCD43C4) is good—R^2 and RMSE of 0.96 and 5.23 days for SOS, 0.77 and 9.23 days for EOS and 0.89 and 12.37 days for LOS, respectively. Similarly, reasonable agreement is seen for SOS ($R^2 = 0.74$) and LOS ($R^2 = 0.59$) between NDVI3g and the MODIS phenology product (MCD12Q2). However, EOS from NDVI3g tended to be much later (bias = 22.42 days). This could be due to varying data-fitting techniques (Savitzky–Golay versus piecewise logistic) and/or detection methods (amplitude threshold versus curvature; White *et al* 2009, Ganguly *et al* 2010).

GSSNDVI captures the spatiotemporal patterns of productivity metrics derived from the other datasets (table 1). The GSSNDVI explains more than 80% of the spatial variation in the MODIS GPP product (MOD17A3; $R^2 = 0.81$). Additional comparisons with MTE-GPP indicate that GSSNDVI captures both spatial ($R^2 = 0.85$) and temporal ($R = 0.52$) variations in gross primary productivity.

At the continental scale, the SOS metrics from NDVI3g and temperature (PSOS) agree quite well ($R = 0.86$ in EA, $R = 0.80$ in NA, $R = 0.82$ in CP)
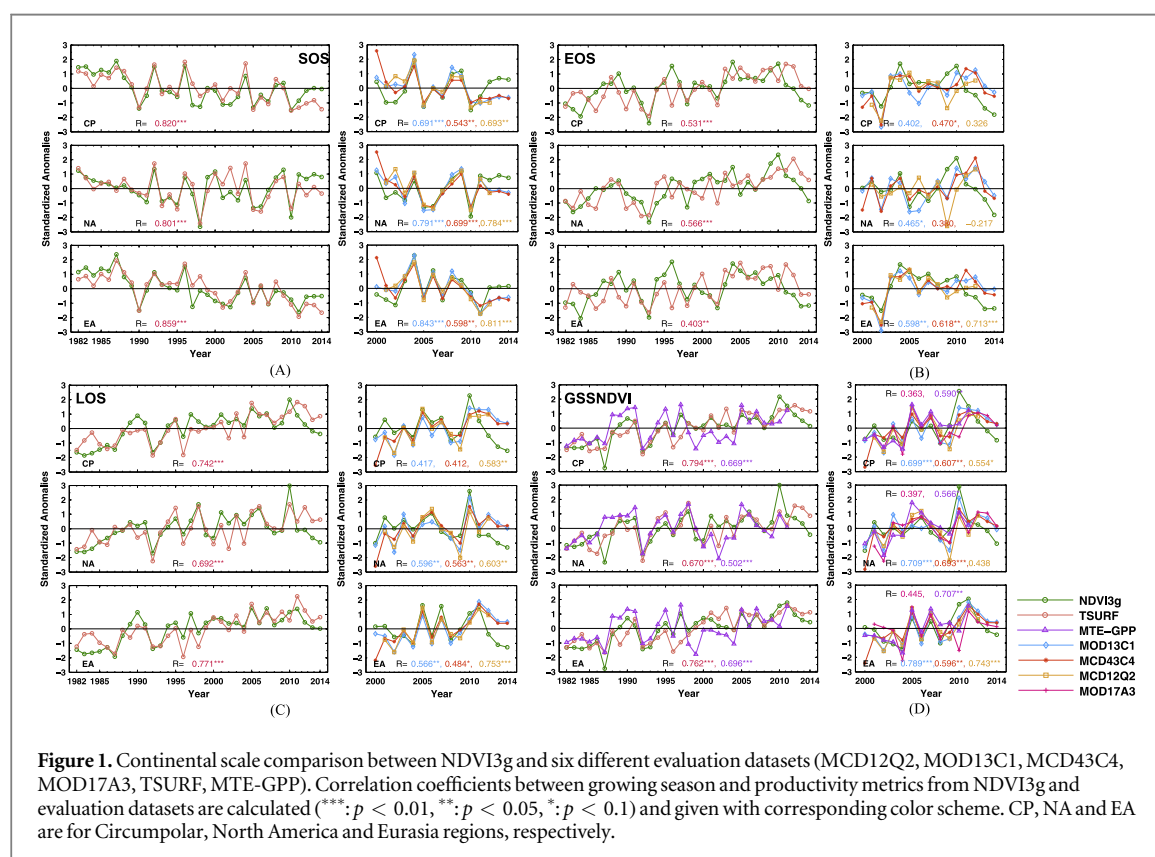
Table 1. Evaluation of NDVI3g based onset of growing season (SOS), end of growing season (EOS), length of growing season (LOS), and growing season summed normalized difference vegetation index (GSSNDVI) at site scale. Respective results of spatial (abbreviated as S) and temporal (abbreviated as T) evaluations are indicated by the coefficient of determination (R^2) and the correlation coefficient (R).

| | NDVI3g | | | | | | | |
| | SOS | | EOS | | LOS | | GSSNDVI | |
	S (R^2)	T (R)	S (R^2)	T (R)	S (R^2)	T (R)	S (R^2)	T (R)
MOD13C1[a]	0.93	0.54	0.78	0.38	0.86	0.44	0.92	0.62
MCD43C4[a]	0.96	0.70	0.77	0.34	0.89	0.50	0.92	0.64
MCD12Q2[b]	0.74	0.58	0.28	0.24	0.59	0.42	0.84	0.50
MOD17A3[c]							0.81	0.48
MTE-GPP[c]							0.85	0.52

[a] NDVI based growing season and productivity (i.e., growing season summed NDVI) derivations.

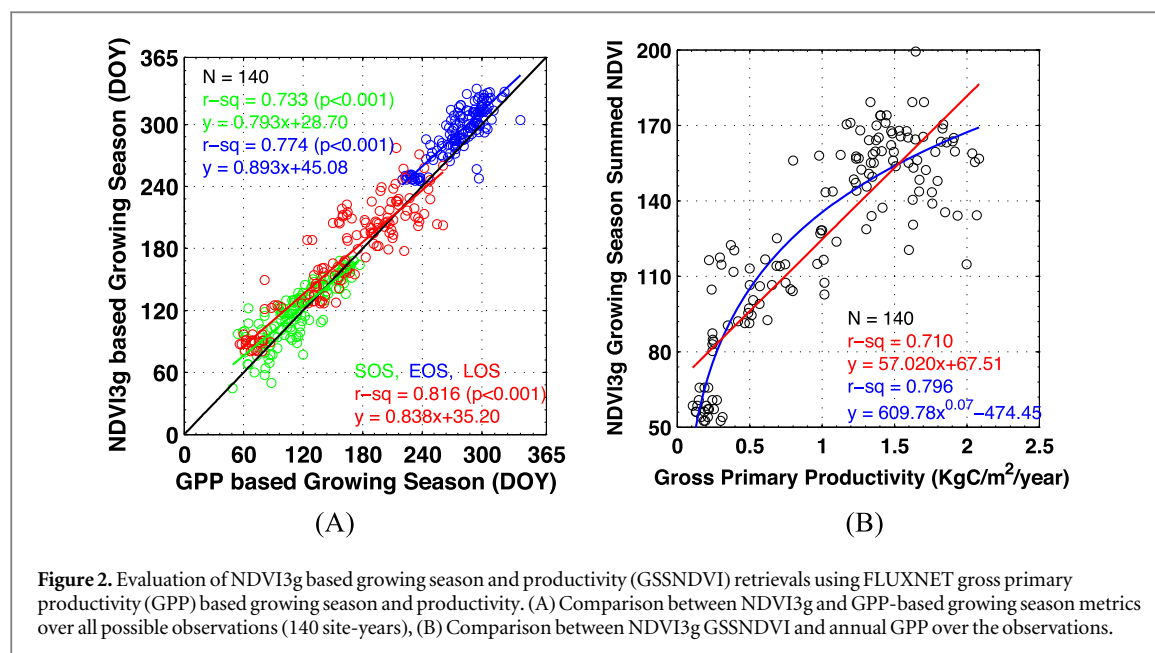[b] EVI based growing season and productivity (i.e., growing season summed EVI) derivations.

[c] Gross primary productivity (GPP) estimate.

Figure 1. Continental scale comparison between NDVI3g and six different evaluation datasets (MCD12Q2, MOD13C1, MCD43C4, MOD17A3, TSURF, MTE-GPP). Correlation coefficients between growing season and productivity metrics from NDVI3g and evaluation datasets are calculated ([***]: $p < 0.01$, [**]: $p < 0.05$, [*]: $p < 0.1$) and given with corresponding color scheme. CP, NA and EA are for Circumpolar, North America and Eurasia regions, respectively.

(figure 1(A)). They show a gradual transition from positive to negative anomalies, thus demonstrating advancing onset of thermal and photosynthetic growing seasons during last three decades. Unlike SOS, the NDVI3g based EOS metric does not exhibit a close correspondence with temperature-based PEOS over last three decades (figure 1(B)). Previous studies have noted that while SOS of northern vegetation is mostly controlled by preseason temperature, EOS has multiple driving factors such as photoperiod, temperature, nutrients, etc (White *et al* 1997, Gill *et al* 2015). Nevertheless, a close association between LOS and PLOS is seen ($R = 0.74$ in CP; figure 1(C)). We also note well-synchronized temporal variations with MODIS LOS

metrics from three different MODIS datasets (MCD12Q2, MOD13C1 and MCD43C4). Overall, NDVI3g based growing season metrics reveal good temporal agreements with those of MODIS although we observed some deviations in later common period (2012∼), particularly for SOS and LOS. This divergence has been caused by the differences in NDVI/EVI response to vegetation growth between sensors, rather than by the processing methods (see detail explanations in figure S3).

GSSNDVI at the circumpolar scale provides a reasonable representation of the long-term MTE-GPP ($R = 0.67$) and GSSWI ($R = 0.79$). Statistically significant strong correlations indicate cumulative

Figure 2. Evaluation of NDVI3g based growing season and productivity (GSSNDVI) retrievals using FLUXNET gross primary productivity (GPP) based growing season and productivity. (A) Comparison between NDVI3g and GPP-based growing season metrics over all possible observations (140 site-years), (B) Comparison between NDVI3g GSSNDVI and annual GPP over the observations.

growing season temperature as the driver of inter-annual and long-term variations in growing season photosynthetic activity. GSSNDVI variations also agree with those seen in four different productivity proxies from MODIS data (figure 1(D)). In particular, productivity proxies based on integral NDVI or EVI over the growing season (MOD13C1, MCD43C4 and MCD12Q2) show relatively stronger correlations than model-based GPP estimates (MOD17A3). This could be due to potentially inaccurate parameterizations in the models and/or uncertainties due to additional meteorological forcing data required by such models (Verma *et al* 2014).

The long-term SOS, EOS, LOS and GSSNDVI anomalies reflect the impact of global climate events such as the eruption of Mt. Pinatubo in 1991 (shorter growing season and decreased productivity) (Lucht *et al* 2002) and the strong El Niño event in 1997–98 (longer growing season and increased productivity) (Buermann *et al* 2003). A particularly prominent feature in these metrics is the intense photosynthetic activity in NA during 2010, which is about three standard deviations above the mean GSSNDVI. This exceptional anomaly in NA is a consequence of the greatest warmth in 2010 (Blunden *et al* 2011) and it is also seen in metrics of MODIS data or other previous studies (Friedl *et al* 2014, Xia *et al* 2015). These matching characteristics features in metrics inferred from data from different sensors are particularly noteworthy.

As for metrics from 36 FLUXNET sites (140 site years), NDVI3g explains 73%, 77% and 82% of variations in SOS, EOS and LOS, respectively (figure 2(A)). NDVI3g SOS and EOS estimates are, on average, 4.2 and 14.6 days later than those inferred from tower GPP data. This translates to a growing season that is 10.5 days longer. Still, NDVI3g data capture the large

variation (60–260 days) in growing season across a range of vegetation types (mixed forests, evergreen needleleaf forests, grasses and tundra) (table S1). Similarly, NDVI3g data capture about 80% of the tower based variations in GPP. However, GSSNDVI tends to saturate and shows large variation when GPP is above $1.5 \text{ kgC m}^{-2} \text{ yr}^{-1}$ (figure 2(B)). This saturation is a well-known behavior of vegetation index data in dense and productive vegetation types (Sellers 1985, Myneni and Williams 1994). The saturation has less impact in our study area because only 3.7% of the vegetation exhibits GSSNDVI greater than 150.

3.2. Long-term changes in growing season over northern lands

The growing season in the north has lengthened, on an average, by 8.58 days over the past 33 years (2.60 d dec^{-1}, $p < 0.05$, table 2). The lengthening is greater in EA than in NA (3.04 versus 1.83 d dec^{-1}, $p < 0.05$). Changes during spring contributed less than changes in autumn to this lengthening in the case of NA. The opposite is the case in EA. Interestingly, changes in growing season duration differed between the first two decades of the data record (1982–1999; 5.06 d dec^{-1}, $p < 0.05$), which was an exceptionally warm period (Trenberth and Fasullo 2013) and the latter part of the data record (2000–2014; -1.08 d dec^{-1}, $p > 0.1$) during which a warming hiatus was noted (table 2). This switch from a lengthened (i.e. advancing SOS and delaying EOS) to a shortened (i.e. delaying SOS and advancing EOS) duration was also reported in other studies (Høgda *et al* 2013, Wang *et al* 2015, Zhao *et al* 2015). However, MODIS indicates lengthening growing season during later period (2000–2014), although the trend estimates from both datasets are not statistically significant from zero ($p > 0.1$) due to the short time-span and large

Table 2. Observed 33 year long-term (1982–2014) growing season and productivity trends over continental scale. Trends over separated 1982–1999 and 2000–2014 periods are also calculated. The trends were evaluated by Vogelsang's *t-PS_T* test. CP, NA and EA are for circumpolar, North America and Eurasia regions, respectively.

	1982–2014			1982–1999			2000–2014		
	CP	NA	EA	CP	NA	EA	CP	NA	EA
SOS (d dec^{-1})	−1.61**	−0.13	−2.45**	−3.67**	−3.20	−3.93**	0.85	2.33	0.00
EOS (d dec^{-1})	0.67*	1.20*	0.36	1.22	0.78	1.46	−0.69	−0.56	−0.76
LOS (d dec^{-1})	2.60**	1.83**	3.04**	5.06*	4.74	5.24*	−1.08	−2.30	−0.38
GSSNDVI (dec^{-1})	2.97***	2.32***	3.34***	4.23*	3.31*	4.75*	1.87	1.65	2.00

Note: ***: $p < 0.01$, **: $p < 0.05$, *: $p < 0.1$.

inter-annual variations (table S2). Interestingly, at least of the same signs are reported when observed abrupt divergence is ignored.

About 30.6% of northern vegetated land shows statistically significant (Vogelsang's *t-PS_T* test at 10% significance level) changes in SOS over the past 33 years (figure 3(A) and table S3). A majority of these (27.9%) shows an advancing SOS trend, that is, a trend towards earlier springtime greening. Only 2.7% show the opposite trend. The former is especially pronounced in EA while the latter is seen mostly in boreal NA. However, the degree of advancing trend in SOS over the boreal region (Max. PDFs in EA: −2.8 d dec^{-1}, NA: −3.0 d dec^{-1}) is relatively higher than in the arctic (Max. PDFs EA: −2.5 d yr^{-1}, NA: −2.3 d dec^{-1}). This pattern was reported by previous studies (Shen *et al* 2014, 2015) and it implies that an earlier SOS in a warmer region may have higher temperature sensitivity than those in a colder region. Reported less sensitive green-up response in arctic vegetation also possibly associates with increasing snowfall in winter/spring time which may hinder much earlier green-up in warmer arctic (e.g., Bieniek *et al* 2015).

About 21.9% of the study region displays a significant delay in autumn senescence (EOS) over the 33 year period of record (figure 3(B) and table S3). The opposite is seen in about 7.8% of the study area. Boreal regions in both NA and EA show predominant delaying EOS, however, the patterns vary between arctic regions in the two continents. Large proportions (>75% of significant changes) of arctic NA show the delayed EOS trend. In EA, this is observed in only about 25% of the vegetated arctic region showing significant changes. These trends in spring greening and autumn senescence resulted in nearly 33% of the northern vegetation experiencing a lengthened growing season (figure 3(C) and table S3). In most such regions, the longer growing season was due to earlier spring time greening. As shown in figure 3(C), trends in LOS over boreal regions in both continents (Max. PDFs in EA: 3.50 d dec^{-1}, NA: 3.75 d dec^{-1}) have relatively greater lengthening rate than those in arctic regions (Max. PDFs in EA: 2.25 d dec^{-1}, NA: 3.25 d dec^{-1}).

3.3. Long-term changes in productivity over northern lands

The analysis indicates that GSSNDVI, a measure of seasonal gross primary productivity, has increased by 2.97 dec^{-1} ($p < 0.01$) over the circumpolar region. The rate of increase in NA (2.32 dec^{-1}, $p < 0.01$) is less than in EA (3.34 dec^{-1}, $p < 0.01$) since the early 1980s (table 2). GSSNDVI exhibits a continuously increasing trend throughout this period, unlike the growing season metrics which show opposite trends between the early (1982–1999) and later (2000–2014) periods of the data record. However, the GSSNDVI trend during the later period (1.87 dec^{-1}, $p > 0.1$) is lower than in the earlier period (4.23 dec^{-1}, $p > 0.05$). These results are concordant between AVHRR based NDVI3g data and MODIS NDVI data (table S2).

About 44.4% of the northern vegetated lands exhibit significant changes ($p < 0.1$). 42.0% of the area experience increasing (greening) GSSNDVI trends (figure 4(A) and table 3). Only a small proportion displays decreasing trend (browning, 2.5%). The greening is more prominently observed in North American mixed forests to the east and arctic coastal tundra and in Eurasian needle-leaf and mixed forests, shrub lands and tundra. A fragmented pattern of greening and browning, mostly over evergreen needle-leaf forest and the forest-shrub ecotone, is seen in the NA boreal region, unlike its counterpart in EA, which shows widespread contiguous greening. This fragmented browning in the interior NA has been reported as consequences of increasing drought stress and fire disturbance (Goetz *et al* 2005, Beck *et al* 2011).

For a large browning area located in the east Bering coast of Alaska (figure 4(A)), according to Bieniek *et al* (2015), this may be linked to delayed snow melt due to increased snow depth in the late winter/early spring as well as increased cloud cover during midsummer. Another large patch of decreasing productivity is prominently seen in the central Siberian plateau (figure 4(A)) which is mostly composed by open larch forest, shrub and erect shrub tundra. This declined productivity is mostly due to the anthropogenic influence (i.e., Cu–Ni smelters) (Toutoubalina and Rees 1999). And smaller areas with such a decline are also found around similar smelters in Kola Peninsula in western part of Russia (Tømmervik *et al* 2003).
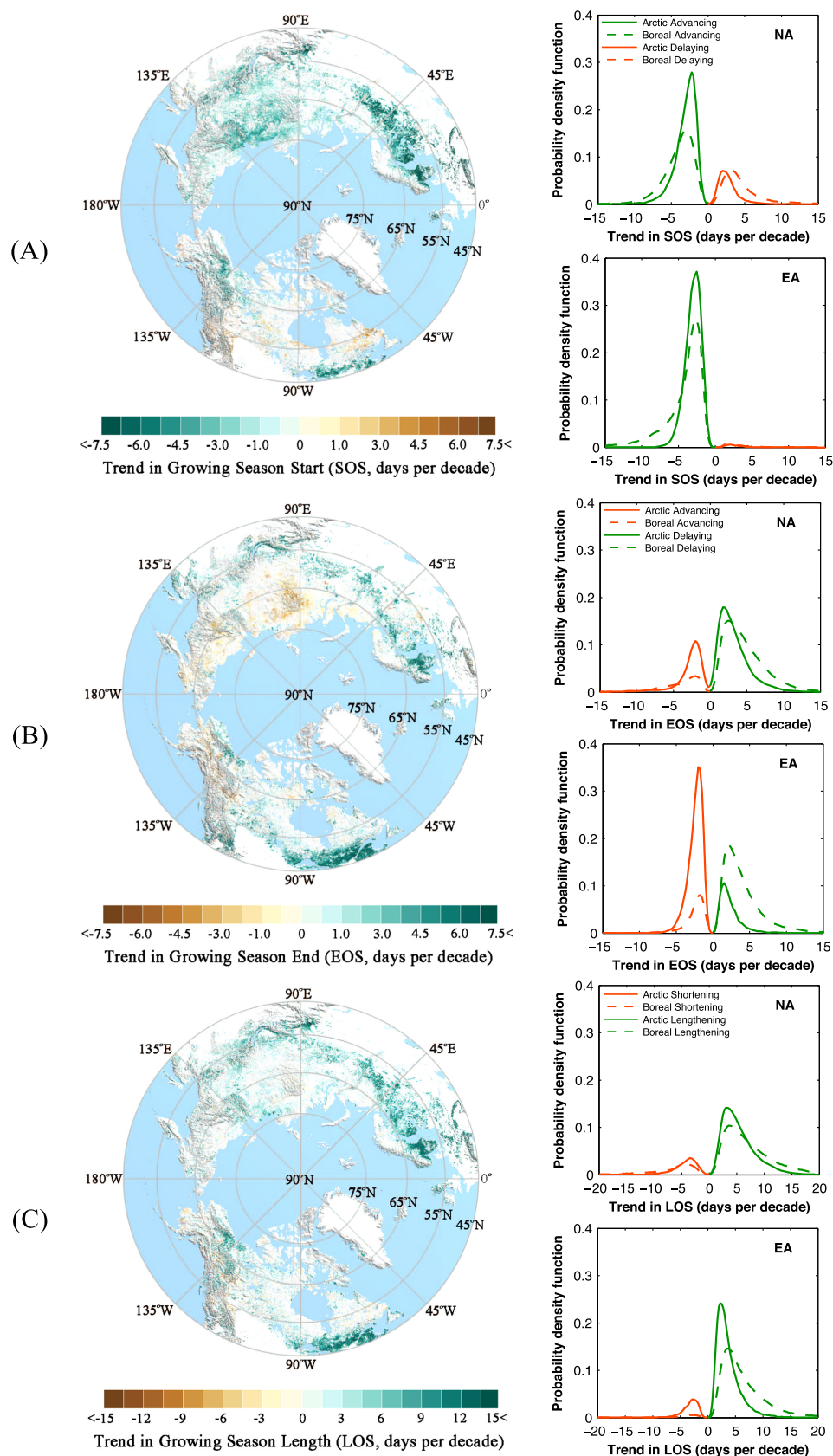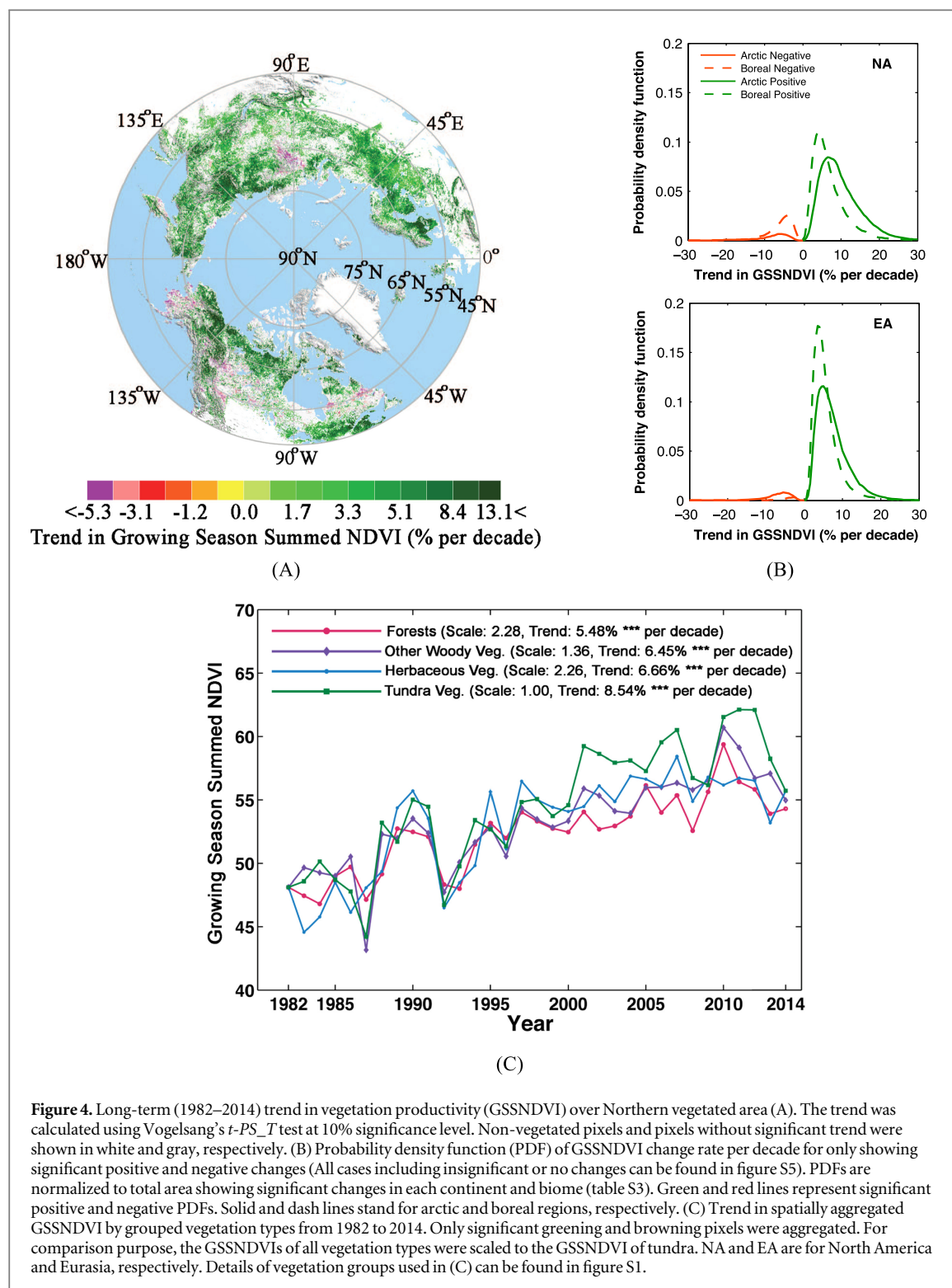
Figure 3. Long-term (1982–2014) trends in vegetation growing season onset (SOS, (A)), end (EOS, (B)) and length (LOS, (C)). The trend was calculated using Vogelsang's *t-PS_T* test at 10% significance level. Non-vegetated pixels and pixels without significant trend were shown in white and gray, respectively. Probability density function (PDF) of change rate per decade for only significant positive and negative changes is also provided (all cases including insignificant or no changes can be found in figure S5). PDFs are normalized to total area showing significant changes in each continent and biome (table S3). NA and EA are for North America and Eurasia. In PDFs, green and red lines represent significant positive and negative changes. Solid and dash lines stand for arctic and boreal regions, respectively.

Figure 4. Long-term (1982–2014) trend in vegetation productivity (GSSNDVI) over Northern vegetated area (A). The trend was calculated using Vogelsang's *t-PS_T* test at 10% significance level. Non-vegetated pixels and pixels without significant trend were shown in white and gray, respectively. (B) Probability density function (PDF) of GSSNDVI change rate per decade for only showing significant positive and negative changes (All cases including insignificant or no changes can be found in figure S5). PDFs are normalized to total area showing significant changes in each continent and biome (table S3). Green and red lines represent significant positive and negative PDFs. Solid and dash lines stand for arctic and boreal regions, respectively. (C) Trend in spatially aggregated GSSNDVI by grouped vegetation types from 1982 to 2014. Only significant greening and browning pixels were aggregated. For comparison purpose, the GSSNDVIs of all vegetation types were scaled to the GSSNDVI of tundra. NA and EA are for North America and Eurasia, respectively. Details of vegetation groups used in (C) can be found in figure S1.

As shown in figure 4(B), arctic vegetation in both NA and EA (Max. PDFs EA: 5.0% dec^{-1}, NA: 6.5% dec^{-1}) displays relatively greater greening rates (with respect to 1982) than boreal vegetation (Max. PDFs EA: 3.5% dec^{-1}, NA: 4.0% dec^{-1}). The areal proportion of boreal browning is dominant (67.9% of browning area in CP) in the northern lands. In particular, North American boreal vegetation accounts for 55.6% of the browning area in the circumpolar region.

The seasonal maximum value of NDVI (MAX) determines the seasonal trajectory of photosynthetic activity. Thus, examining changes in MAX helps to better understand spatiotemporal changes in GSSNDVI. The spatial distribution of statistically significant increasing trends in MAX, shown in figure S4, closely resembles that of GSSNDVI (figure 4(A)), especially in the coastal arctic regions. Whereas resembled trend pattern between GSSNDVI and growing season

Table 3. Area and productivity (GSSNDVI) changes of vegetation classes showing statistically significant (10% level) trend in GSSNDVI. The trends were calculated pixel by pixel from GSSNDVI between 1982 and 2014 using the Vogelsang model.

Vegetation class	Area				Productivity (GSSNDVI)	
	G (%)	B (%)	N (%)	T (%)	I (%)	D (%)
Mixed Forests	10.43	0.10	7.03	17.56	6.12	−0.06
Deciduous Needleleaf Forests	3.67	0.07	5.36	9.10	1.40	−0.02
Evergreen Needleleaf Forests	8.10	0.71	12.01	20.82	4.93	−0.47
Forest-Shrubs Ecotone	4.01	0.51	7.91	12.43	1.81	−0.22
Closed Shrublands	0.16	0.01	0.21	0.38	0.08	−0.01
Open Shrublands	9.72	0.71	14.41	24.84	4.11	−0.28
Grasslands/Wetlands (North of Forests)	0.35	0.02	0.88	1.25	0.25	−0.02
Erect Shrub Tundra	2.41	0.11	2.48	5.00	1.01	−0.06
Prostrate Shrub Tundra	0.57	0.04	1.30	1.91	0.18	−0.01
Graminoid Tundra	2.13	0.12	3.11	5.36	0.87	−0.05
Wetlands	0.41	0.08	0.88	1.37	0.17	−0.04
Total	41.96	2.48	55.56	100.00	20.92	−1.23

Note. For area changes, positive trends indicate greening (abbreviated as G), negative trends indicate browning (abbreviated as B) and no-change (abbreviated as N). Also, total area of each vegetation classes is given (abbreviated as T). For productivity change, productivity increase is abbreviated as I; productivity decrease is abbreviated as D. Productivity change columns show the change in productivity (%) over the area only showing significant changes (positive or negative) between 1982 and 2014. The changes were calculated by $\dfrac{100 \times \sum_{p=1}^{\mathrm{NVC}_i} 33 \text{ yr} \cdot T_p \cdot A_p}{G_{1982} + B_{1982}}$, where NVC$_i$ is the total pixel number of the ith vegetation classes showing significant positive or negative changes, T_p is the yearly common productivity trend (yr^{-1}) of pixel p, A_p is the area weight (unitless) of pixel p, G_{1982} (=9.04 × 10^8, unitless) and B_{1982} (=5.89 × 10^7, unitless) are the total GSSNDVI of greening pixels and total GSSNDVI of browning pixels in 1982 (table S4). Total vegetated area is about 26.02 million km^2.

duration (figure 3(C)) can be found in relatively warmer vegetated area. This implies that the seasonal maximum productivity and growing season duration jointly control inter-annual variation and trend of GSSNDVI with differently characterized relative contributions (Xia *et al* 2015).

Figure 4(C) displays the GSSNDVI time series of four different vegetation groups. The GSSNDVI of forests, other woody vegetation and herbaceous vegetation are scaled to the GSSNDVI of tundra for comparison purposes. All four vegetation groups show increasing GSSNDVI trends with tundra exhibiting the largest trend (8.5% dec^{-1}) and forests displaying the lowest (5.5% dec^{-1}). This reflects the higher sensitivity of tundra vegetation productivity as compared to boreal forests (Verbyla 2008, Beck and Goetz 2011). There is considerable variation in the trajectory of these time series and the declining greening rate can be clearly seen after the late 1990s. These flattened or slowed change rates are coincident with recently observed warming deceleration (Trenberth and Fasullo 2013) and divergent vegetation growth responses imply differently characterized sensitivities to changing climate. For instance, continued warming may appear to no longer promote boreal forest growth, while the warming may benefit tundra growth (Beck and Goetz 2011, Bi *et al* 2013).

Our analysis indicates that 42.0% of the total northern vegetated area shows a greening trend over past three decades (table 3). This translates to a 20.9%

gain in productivity since 1982. In contrast, the 2.5% of browning regions resulted in a decrease of about 1.2% of gross primary productivity since 1982. Note that the quantities of productivity changes represent only regions showing significant directional changes. All forests, in particular the mixed and evergreen needleaf forests, contributed significantly to the observed gains in productivity. Equally noteworthy is the contribution of shrublands and the forest-shrub ecotone to productivity gains in view of the large greening extent observed in these vegetation types (table 3).

4. Concluding remarks

We investigated changes in metrics of growing season (SOS, EOS and LOS) and gross primary productivity (GSSNDVI) over the boreal and arctic lands using long-term satellite observations (GIMMS NDVI3g). An accurate derivation of growing season duration from satellite data is a challenging task. Also, the vegetation index data accumulated over the derived growing season must reflect gross primary productivity. In this sense, the main discriminating point of this work is threefold: (1) this study introduced the photosynthetically active growing season definition by combining optically measured vegetation greenness and ground freeze/thaw data to properly demonstrate photosynthetic activities in northern vegetation. (2) Moreover, we incorporated yearly varying growing season to productivity characterization, thus we enable

to understand the relative contribution of growing season and peak greenness on annual gross productivity variability. (3) We evaluated retrieved growing season and productivity metrics using independent multiple direct and indirect measures, particularly eddy-covariance measurements encompassing a wide range of biomes and regions. Special emphasis was placed on assuring that the derived metrics were accurate by comparing them to several independent direct and indirect reference data sets. Overall, these inter-comparison and evaluation analyses reflected that the metrics derived from NDVI3g were reasonably accurate at a range of spatio-temporal scales. Statistical analyses presented in this article provided comprehensive information about patterns in inter-annual variations and long-term trends over the past three decades. At the hemispheric scale, we observed a significant advance in SOS, delay in EOS and lengthened LOS, all of which are concordant with thermal growing season variations. The longer growing season and increasing photosynthetic activity resulted in a predominant greening trend over 42.0% of the northern vegetated area. This translated to a 20.9% gain in gross primary productivity during last three decades. The GSSNDVI exhibited a continuously increasing trend throughout the 1982–2014 period, unlike the growing season metrics which showed opposite trends between the early (1982–1999) and later (2000–2014) periods of the data record. The arctic and boreal regions showed surprisingly different variations— greater rate of productivity change and smaller rate of growing season duration change in the arctic versus the opposite in the boreal vegetation—perhaps reflective of the biome-specific temperature sensitivity of the vegetation. Together these results document large-scale spatio-temporal changes happening in the northern vegetation.

Acknowledgments

References

Baret F *et al* 2006 Evaluation of the representativeness of networks of sites for the global validation and intercomparison of land biophysical products: proposition of the CEOS-BELMANIP *IEEE Trans. Geosci. Remote* **44** 1794–803

Beck P S *et al* 2006 Improved monitoring of vegetation dynamics at very high latitudes: a new method using MODIS NDVI *Remote Sens. Environ.* **100** 321–34

Beck P S *et al* 2011 Changes in forest productivity across Alaska consistent with biome shift *Ecol. Lett.* **14** 373–9

Beck P S and Goetz S J 2011 Satellite observations of high northern latitude vegetation productivity changes between 1982 and 2008: ecological variability and regional differences *Environ. Res. Lett.* **6** 045501

Bi J *et al* 2013 Divergent arctic-boreal vegetation changes between North America and Eurasia over the past 30 years *Remote Sens.* **5** 2093–112

Bieniek P A *et al* 2015 Climate drivers linked to changing seasonality of Alaska coastal tundra vegetation productivity *Earth Interact.* **19** 1–29

Bjerke J W *et al* 2014 Record-low primary productivity and high plant damage in the Nordic Arctic Region in 2012 caused by multiple weather events and pest outbreaks *Environ. Res. Lett.* **9** 084006

Blunden J *et al* 2011 State of the climate in 2010 *Bull. Am. Meteorol. Soc.* **92** S1–266

Buermann W *et al* 2003 Interannual covariability in Northern Hemisphere air temperatures and greenness associated with El Niño-Southern Oscillation and the Arctic Oscillation *J. Geophys. Res. Atmos.* **108** 4396

Chapin F *et al* 2000 Arctic and boreal ecosystems of western North America as components of the climate system *Glob. Change Biol.* **6** 211–23

Chen J *et al* 2004 A simple method for reconstructing a high-quality NDVI time-series data set based on the Savitzky–Golay filter *Remote Sens. Environ.* **91** 332–44

Forkel M *et al* 2016 Enhanced seasonal CO_2 exchange caused by amplified plant productivity in northern ecosystems *Science* **351** 696–9

Friedl M A *et al* 2010 MODIS Collection 5 global land cover: algorithm refinements and characterization of new datasets *Remote Sens. Environ.* **114** 168–82

Friedl M A *et al* 2014 A tale of two springs: using recent climate anomalies to characterize the sensitivity of temperate forest phenology to climate change *Environ. Res. Lett.* **9** 054006

Ganguly S *et al* 2010 Land surface phenology from MODIS: characterization of the collection 5 global land cover dynamics product *Remote Sens. Environ.* **114** 1805–16

Gill A L *et al* 2015 Changes in autumn senescence in northern hemisphere deciduous trees: a meta-analysis of autumn phenology studies *Ann. Bot.* **116** 875–88

Goetz S J *et al* 2005 Satellite-observed photosynthetic trends across boreal North America associated with climate and fire disturbance *P. Natl Acad. Sci. USA* **102** 13521–5

Goward S N, Tucker C J and Dye D G 1985 North American vegetation patterns observed with the NOAA-7 advanced very high resolution radiometer *Vegetatio* **64** 3–14

Høgda K A *et al* 2013 Trends in the start of the growing season in Fennoscandia 1982–2011 *Remote Sens.* **5** 4304–18

Jönsson P and Eklundh L 2004 TIMESAT–a program for analyzing time-series of satellite sensor data *Comput. Geosci.* **30** 833–45

Keenan T F *et al* 2014 Net carbon uptake has increased through warming-induced changes in temperate forest phenology *Nat. Clim. Change* **4** 598–604

Lucht W *et al* 2002 Climatic control of the high-latitude vegetation greening trend and Pinatubo effect *Science* **296** 1687–9

Mann H B 1945 Nonparametric tests against trend *Econometrica* **13** 245–59

Menzel A *et al* 2006 European phenological response to climate change matches the warming pattern *Glob. Change Biol.* **12** 1969–76

Myneni R *et al* 1997 Increased plant growth in the northern high latitudes from 1981 to 1991 *Nature* **386** 698

Myneni R and Williams D 1994 On the relationship between FAPAR and NDVI *Remote Sens. Environ.* **49** 200–11

Nemani R R *et al* 2003 Climate-driven increases in global terrestrial net primary production from 1982 to 1999 *Science* **300** 1560–3

Parmesan C and Yohe G 2003 A globally coherent fingerprint of climate change impacts across natural systems *Nature* **421** 37–42

Pettorelli N *et al* 2005 Using the satellite-derived NDVI to assess ecological responses to environmental change *Trends Ecol. Evol.* **20** 503–10

Piao S *et al* 2011 Changes in satellite-derived vegetation growth trend in temperate and boreal Eurasia from 1982 to 2006 *Glob. Change Biol.* **17** 3228–39

Pinzon J E and Tucker C J 2014 A non-stationary 1981–2012 AVHRR NDVI3g time series *Remote Sens.* **6** 6929–60

Richardson A D *et al* 2010 Influence of spring and autumn phenological transitions on forest ecosystem productivity *Phil. Trans. R. Soc.* B **365** 3227–46

Richardson A D *et al* 2013 Climate change, phenology, and phenological control of vegetation feedbacks to the climate system *Agric. Forest. Meteorol.* **169** 156–73

Sellers P J 1985 Canopy reflectance, photosynthesis and transpiration *Int. J. Remote Sens.* **6** 1335–72

Serreze M *et al* 2000 Observational evidence of recent change in the northern high-latitude environment *Clim. Change* **46** 159–207

Shen M *et al* 2014 Earlier-season vegetation has greater temperature sensitivity of spring phenology in Northern Hemisphere *PloS One* **9** e88178

Shen M, Cong N and Cao R 2015 Temperature sensitivity as an explanation of the latitudinal pattern of green-up date trend in Northern Hemisphere vegetation during 1982–2008 *Int. J. Climatol.* **35** 3707–12

Solomon S 2007 *Climate Change 2007-the Physical Science Basis: Working Group I Contribution to the Fourth Assessment Report of the IPCC* (Cambridge: Cambridge University Press)

Tape K, Sturm M and Racine C 2006 The evidence for shrub expansion in northern Alaska and the Pan-Arctic *Glob. Change Biol.* **12** 686–702

Toutoubalina O V and Rees W G 1999 Remote sensing of industrial impact on Arctic vegetation around Noril'sk, northern Siberia: preliminary results *Int. J. Remote Sens.* **20** 2979–90

Trenberth K E and Fasullo J T 2013 An apparent hiatus in global warming? *Earth's Future* **1** 19–32

Tucker C J 1979 Red and photographic infrared linear combinations for monitoring vegetation *Remote Sens. Environ.* **8** 127–50

Tømmervik H, Høgda K A and Solheim I 2003 Monitoring vegetation changes in Pasvik (Norway) and Pechenga in Kola Peninsula (Russia) using multi-temporal Landsat MSS/TM data *Remote Sens. Environ.* **85** 370–88

Verbyla D 2008 The greening and browning of Alaska based on 1982–2003 satellite data *Glob. Ecol. Biogeogr.* **17** 547–55

Verma M *et al* 2014 Remote sensing of annual terrestrial gross primary productivity from MODIS: an assessment using the FLUXNET La Thuile data set *Biogeosciences* **11** 2185–200

Vogelsang T J 1998 Trend function hypothesis testing in the presence of serial correlation *Econometrica* **66** 123–48

Walker D A *et al* 2005 The circumpolar Arctic vegetation map *J. Veg. Sci.* **16** 267–82

Walther G R *et al* 2002 Ecological responses to recent climate change *Nature* **416** 389–95

Wang J *et al* 2004 Relations between NDVI and tree productivity in the central Great Plains *Int. J. Remote Sens.* **25** 3127–38

Wang X *et al* 2015 Has the advancing onset of spring vegetation green-up slowed down or changed abruptly over the last three decades? *Global Ecol. Biogeogr.* **24** 621–31

White M A *et al* 2009 Intercomparison, interpretation, and assessment of spring phenology in North America estimated from remote sensing for 1982–2006 *Global Change Biol.* **15** 2335–59

White M A, Thornton P E and Running S W 1997 A continental phenology model for monitoring vegetation responses to interannual climatic variability *Glob. Biogeochem. Cycles* **11** 217–34

Xia J *et al* 2015 Joint control of terrestrial gross primary productivity by plant phenology and physiology *Proc. Natl Acad. Sci. USA* **112** 2788–93

Xu L *et al* 2013 Temperature and vegetation seasonality diminishment over northern lands *Nat. Clim. Change* **3** 581–6

Zhao J *et al* 2015 Spatial and temporal changes in vegetation phenology at middle and high latitudes of the Northern Hemisphere over the past three decades *Remote Sens.* **7** 10973–95

Zhu Z *et al* 2016 Greening of the Earth and its drivers *Nat. Clim. Change* (doi:10.1038/nclimate3004)